2017 2nd International Conference on Civil Engineering and Rock Engineering (ICCERE 2017)
ISBN: 978-1-60595-513-1

Variations in Crack Features of Granite Specimen During Laboratory Uniaxial Compression Test Using Image Processing

Yongdong Wang, Jinming Xu and Xinyu Cao

ABSTRACT

The granite is a heterogeneous rock consisting of various microscopic compositions (i.e., quartz, feldspar, biotite, etc). Changes in the digital features of these compositions are important in understanding the deformation and failure mechanisms of the rock. The video images photographed during the uni-axial compression test were used to investigate the digital changes of the cracks in the rock. The original images were first transferred into the gray and binary ones using the digital image processing. The positions of cracks were extracted using the grayscale threshold segmentation and traditional visual identification. The changes in the digital features of the cracks were furthermore explored in various stages during the specimen failure. It shows that the failure process of the granite specimen may be divided into three stages, or, stable, speeded, and complete ones; at the stable stage, the first crack initiates and propagates gradually with the great changes in the crack features; at the speeded stage, two of new cracks generate and all of cracks propagate much quickly; at the complete failure stage, all of the cracks changes gradually again until the rock approached to failure. The results presented herein may be referable in investigating the failure mechanism of the rock material. [1] [2] [3]

[1] Yongdong Wang, Hongyuan Science and Technology Corporation Limited of Construction Engineering, Shanghai 201707, China.
[2]Jinming Xu, Department of Civil Engineering, Shanghai University, Shanghai 200444, China.
[3]Xinyu Cao, Department of Civil Engineering, Shanghai University, Shanghai 200444, China.

INTRODUCTION

Variations in crack features of a rock are of great importance in understanding the failure process of the material. In conventional methods, this process is examined usually by analyzing the specimen appearances in the laboratory tests.

From the observations in the laboratory tests, it is known that the crack initiates usually in the matrix (Amann et al [1]; Ündül et al [2]). The crack propagation are much dependant on the stress magnitude, micro-damage localization and mineralogical features such as type, percentage, and microstructure (Amann et al [1]; Ündül et al [2]; Lin and Labuz [3]), and eventually change the strength of rocks. The orientation, velocity, and length of crack propagation are much related to the crack types (Rigopoulos et al [4]).

To obtain more details in crack initiation and propagation, the image processing techniques were performed (Rigopoulos et al [4]). The related displacements were exactly measured using digital image correlation (Lin and Labuz [3]). The video images were used to track the movement of crack by taking crack as tracking targets, and the features (including length, width and area) of the various constituents during the crack initiation and propagation process were also investigated (Xu et al [5]).

Nevertheless, the crack features during the failure process of the rock materials are not clear. In the current study, the test video images photographed during laboratory uni-axial compression test were used to investigate the changes in various features of cracks. The locations of cracks were monitored by using the grayscale segmentation techniques. The digital features of the cracks were represented by the length, width, and areas. The changes of the crack features with the failure process were thereafter examined.

RECOGNITION OF CRACKS USING TEST VIDEO IMAGE

Test Video Image And Pre-processing

The rock type used in the current study is the Baishan granite, located in Gansu Province, China. The granite is composed of feldspar, quartz and biotite. The rock was sliced and polished into the specimens with the size of around 50 mm × 50 mm × 100 mm in laboratory. The uni-axial compression tests for the specimens were performed using a hydraulic machine. The stress-strain data on the plate were acquired using the computer-controlled system.

During the laboratory tests, the video images were photographed using a digital camera normal to the specimen surface with a distance of about 0.5 m. One of the video images was used here to perform the analyses. The total of the video image occupied 119.1 s with 2978 frames at a rate of 25 frames per second. One frame in the video image continued 0.04 s (1/25 = 0.04).

To be easier in the later processing, the original video image was preprocessed both by the decompression of the original video images into the 24 colorful ones with the AVI format and by the selection of the areas with the cracks in the frames. The original video image was then transferred into one with 100 frames at an interval of 4.00 s.

Recognition of Cracks

For each frame in the test video image, the threshold segmentation technique was used to extract the various compositions (including crack) regions on the specimen surface. Figure 1 show a binary image during the specimen failure.

CRACK FEATURES AT VARIOUS FAILURE STAGES

According to the number and the change speed, the failure process of the specimen was divided into three stages, or, the stable (only one crack appeared), speeded (three cracks appeared and propagated quickly), and complete failure ones (three cracks changes gradually and the rock approached to failure). The crack features in these stages will be described in the following parts.

At Stable Stage

During the stable stage, the variations in external loads with time are shown in Figure 2. The widths, lengths, and areas of the newly-generated crack with time are shown respectively in Figures 3, 4, and 5. It can be seen from Figures 2 to 5 that during the stable stage, the first crack (or crack 2) initiates on the specimen surface at the frame 25 (or 219.1 s) and the crack propagates gradually and lasts 0.6 s when the load decrease with time at an interval.

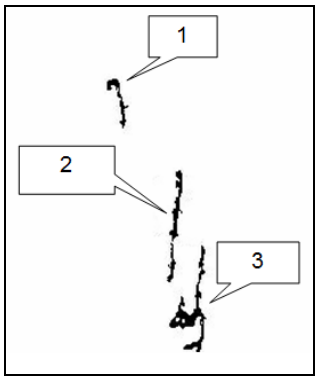

Figure 1. A binary image during failure of granite specimen.

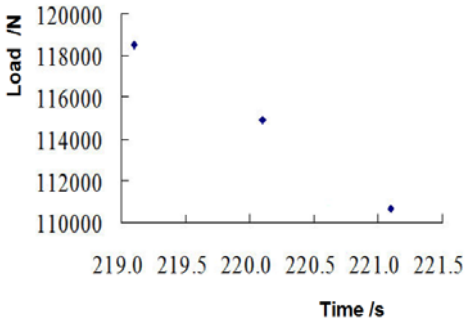

Figure 2. Variations in loads with time at stable stage.

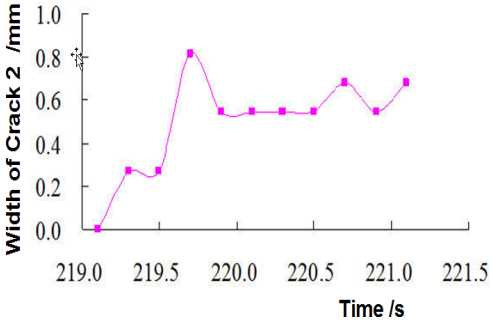

Figure 3. Variations in widths of crack 2 with time at stable stage.

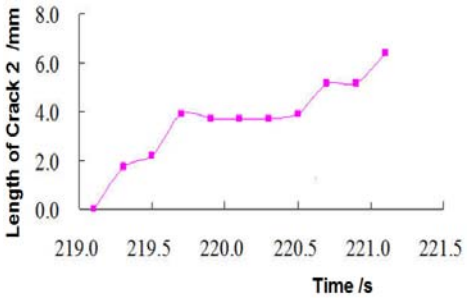

Figure 4. Variations in lengths of crack 2 with time at stable stage.

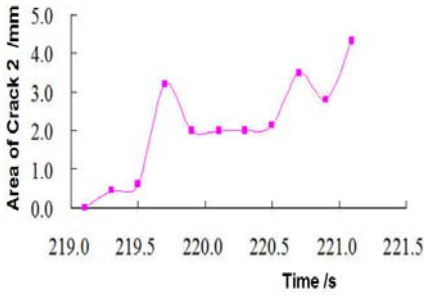

Figure 5. Variations in areas of crack 2 with time at stable stage.

At the instant of 219.7 s, the width of the crack 2 increases into the peak value of 0.82 mm; afterwards, this width decreases into the value of around 0.54 mm (or decreased by 34.15%) and tends to be stable. The lengths of the crack 2, nevertheless, increase with time and reach to the peak at 221.1 s. The areas of the crack 2 increase with time at the beginning and reach to the first peak value of 3.19 mm² at 219.7 s, then decrease gradually with time at an interval of 0.4 s, and increase again with time by reaching to the peak value of 4.32 mm².

In summary, the first crack initiates on the specimen surface and propagates gradually with the great changes in the widths, lengths, and areas at the stable stage.

At Speeded Stage

During the speeded stage, cracks 1 and 3 generated. The crack 1, apart from the top crack (or crack 2) with 42 mm, is selected to investigate the changes of the crack features. At this stage, the variations in external loads with time are shown in Figure 6. The widths, lengths, and areas of the crack with time are respectively shown in Figures 7, 8, and 9.

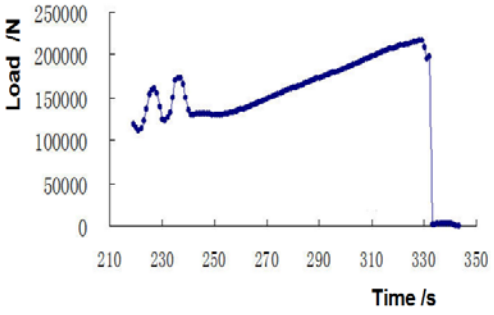

Figure 6. Variations in loads with time at speeded stage.

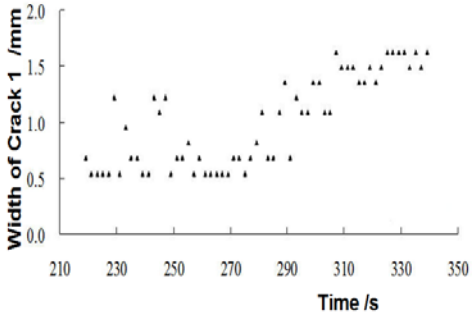

Figure 7. Variations in widths of crack 1 with time at speeded failure stage.

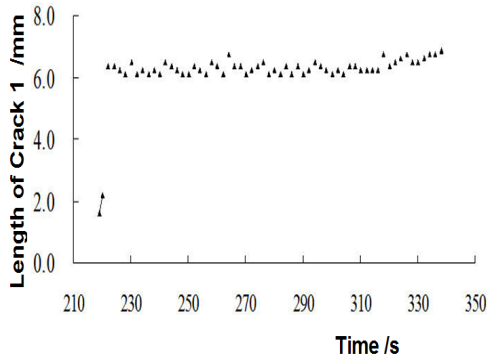

Figure 8. Variations in lengths of crack 1 with time at speeded failure stage.

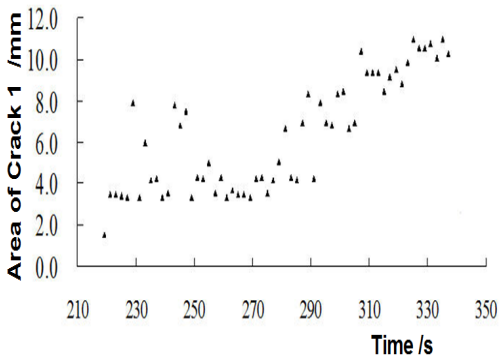

Figure 9. Variations in areas of crack 1 with time at speeded failure stage.

It can be seen from Figures 6 to 9 that at the interval of 221.1 to 340 s, the width of the crack almost unchanged at the beginning, then increased quickly with time at a lag of 3 to 4 s, and reached to the second peak value of 1.63 mm at the instant of 307.1 s; afterwards, the width of the crack decreased to the stable value of around 1.63 mm. The lengths of the crack changed little with a stable value of 6.49 mm. The changes of the crack areas are similar to those of the crack width and reach to the magnitude of around 10.7 mm^2.

It can be also seen that at the interval of 221.1 to 340 s, the width of the crack almost unchanged at the beginning, then increased linearly with time at a lag of 3 to 4 s, and reached to the second peak value of 1.63 mm at the instant of 307.1 s; afterwards, the width of the crack decreased to the stable value of around 1.63 mm. The lengths of the crack changed little with a stable value of 6.49 mm. The changes of the crack areas are similar to those of the crack width and reach to the magnitude of around 10.7 mm^2.

At the speeded stage, in summary, two of new cracks generated and all of cracks propagated much quickly.

At Complete Failure Stage

At this stage, the crack 1 is again selected to investigate the changes in the crack features, focusing on the width changes. The variations in external loads with time are shown in Figure 10. The lengths of the crack with time are shown in Figure 11. The widths of the crack with time at 1.59 and 2.93 mm from the top of crack tip are respectively shown in Figure 12 and Figure 13.

It can be seen from Figure 11 that as the external load decreases at an interval at the complete failure stage, the length of the crack 1 increases gradually, reaches to the peak one (9.30 mm) at 342.6 s, and is then stable up to the completely failure of the specimen.

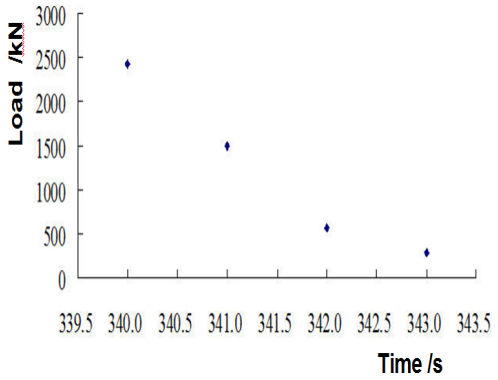

Figure 10. Variations in loads with time at complete failure stage.

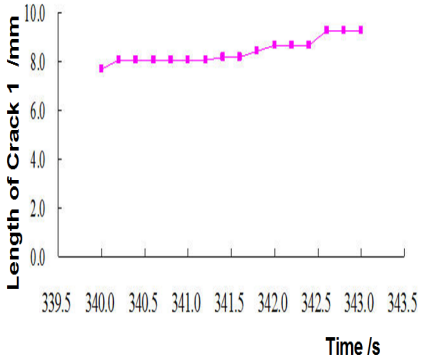

Figure 11. Variations in lengths with time of crack 1 at complete failure stage.

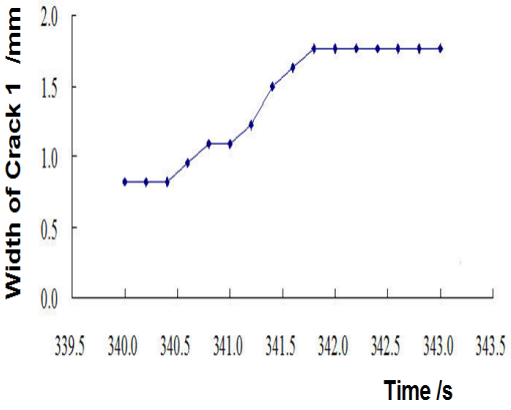

Figure 12. Variations in crack widths with time at 1.59 mm from the top tip of crack 1 at complete failure stage.

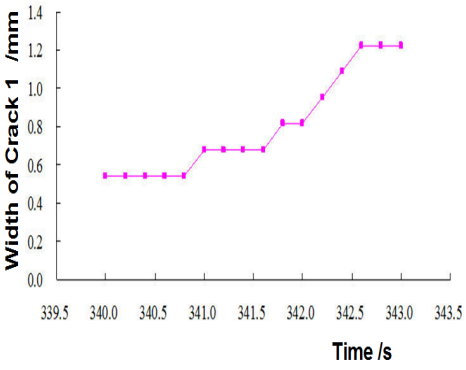

Figure 13. Variations in crack widths with time at 2.93 mm from the top tip of crack 1 at complete failure stage.

From Figures 12 and 13, It can be seen that the width of the crack 1 at 1.59 mm from the top of crack tip is 0.82 mm as appears at 340 s; afterwards, the external load decreases, whereas the crack width increases gradually, reaches to the peak one (1.77 mm) at 341.8 s, and is then stable up to the completely failure of the specimen. The width of the crack 1 at 2.93 mm from the top of crack tip is 0.54 mm as appears at 340 s; afterwards, the external load decreases, whereas the crack width increases gradually, reaches to the peak one (1.22 mm) at 342.6 s, and is then stable up to the completely failure of the specimen.

At the complete failure stage, in summary, all of the cracks changes gradually until the rock approached to failure, the changes in widths are more quickly at the centered parts.

CONCLUSIONS

(1) Under uni-axial compression, the failure of the granite specimen may be divided into the stable, speeded, and complete stages;

(2) At the stable stage, the first crack initiates and propagates gradually on the specimen surface and has a great change in the width, length, and area;

(3) At the speeded stage, two of the new cracks generated on the surface, and all of cracks propagated much quickly on the specimen;

(4) At the complete failure stage, all of the cracks on the specimen changes gradually until the rock approached to failure, and the changes in widths are more quickly at the centered parts.

ACKNOWLEDGEMENTS

We gratefully thank the financial support provided by the Natural Sciences Foundation Committee of China under Grant No.41472254.

REFERENCES

1. Amann, F., Ündül, Ö., Kaiser, and P.K. 2014. “Crack initiation and crack propagation in heterogeneous sulfate-rich clay rocks”. *Rock Mech. Rock Eng.*, 47: 1849-1865.
2. Ündül, Ö., Amann, F., Aysal, N., and Plötze, M.L. 2015. “Micro-textural effects on crack initiation and crack propagation of andesitic rocks”. *Eng. Geol.*, 193: 267-275.
3. Lin, Q., and Labuz, J.F., 2013. “Fracture of sand stone characterized by digital image correlation”. *Int. J. Rock Mech. Min. Sci.*, 60: 235-245.
4. Rigopoulos, I., Tsikouras, B., Pomonis, P., and Hatzipanagiotou, K. 2013. “Petrographic investigation of microcrack initiation in mafic ophiolitic rocks under uniaxial compression”, *Rock Mech. Rock Eng.*, 46: 1061-1072.
5. Xu, J., Liu, F., Chen, Z., and Wu, Y. 2017. “Digital features of main constituents in granite during crack initiation and propagation”. *Eng. Geol.*, 225: 96-102.